Pre-Clinical Research Report

Journal of INTERNATIONAL MEDICAL RESEARCH

Journal of International Medical Research
2018, Vol. 46(7) 2883–2897

DOI: 10.1177/0300060518778711
journals.sagepub.com/home/imr
SAGE

Astragaloside IV ameliorates early diabetic nephropathy by inhibition of MEK1/2-ERK1/2-RSK2 signaling in streptozotocin-induced diabetic mice

Gaofeng Song[1,*], Pengxun Han[1,*], Huili Sun[1], Mumin Shao[2], Xuewen Yu[2], Wenjing Wang[1], Dongtao Wang[1], Wuyong Yi[1], Na Ge[1], Shunmin Li[1,*] and Tiegang Yi[1]

Abstract

Objective: The aim of this study was to investigate the renoprotective effects and molecular mechanisms of astragaloside IV (AS-IV) in streptozotocin (STZ)-induced diabetic mice.

Methods: Male C57BL/6 mice were injected intraperitoneally with STZ at 200 mg/kg body weight. AS-IV was administered for 8 consecutive weeks, beginning 1 week after STZ injection. Body weight, 24-hour urinary albumin excretion, and fasting blood glucose were measured. Kidney tissues were examined by histopathological analyses. Total levels and phosphorylation of mitogen-activated protein kinase 1/2 (MEK1/2), extracellular signal-regulated kinases 1 and 2 (ERK1/2), and ribosomal S6 kinase 2 (RSK2) were determined by Western blotting analysis.

Results: AS-IV treatment significantly reduced albuminuria and serum creatinine levels, ameliorated mesangial matrix expansion and greater foot process width, and decreased the levels of urinary N-acetyl-beta-D-glucosaminidase, neutrophil gelatinase-associated lipocalin, and transforming growth factor-beta 1 in STZ-induced diabetic mice. AS-IV also inhibited renal cortical phosphorylation of MEK1/2, ERK1/2 and RSK2.

[1]Department of Nephrology, Shenzhen Traditional Chinese Medicine Hospital, The Fourth Clinical Medical College of Guangzhou University of Chinese Medicine, Shenzhen, China
[2]Department of Pathology, Shenzhen Traditional Chinese Medicine Hospital, The Fourth Clinical Medical College of Guangzhou University of Chinese Medicine, Shenzhen, China

*These authors contributed equally to this work.

Corresponding author:
Tiegang Yi, Department of Nephrology, Shenzhen Traditional Chinese Medicine Hospital, The Fourth Clinical Medical College of Guangzhou University of Chinese Medicine, 1 Fuhua Road, Futian District, Shenzhen, Guangdong 518033, China.
Email: szyitiegang@126.com

Conclusion: Our results suggest that AS-IV attenuates renal injury in STZ-induced diabetic mice. This effect might be partially associated with inhibition of the activation of the MEK1/2-ERK1/2-RSK2 signaling pathway.

Keywords
Diabetic nephropathy, diabetes, astragaloside, ERK1/2, renal fibrosis, streptozotocin, albuminuria, extracellular matrix, mitogen-activated protein kinase

Date received: 28 October 2017; accepted: 30 April 2018

Introduction

Diabetic nephropathy (DN), one of the most serious microvascular complications associated with diabetes mellitus (DM), has become the predominant cause of end-stage renal disease (ESRD) worldwide.[1–3] The early abnormalities of DN include hyperfiltration and microalbuminuria. These abnormalities are followed by histological and structural changes, including mesangial expansion and thickening of the glomerular basement membrane (GBM).[4] The precise pathogenesis of DN has not yet been fully elucidated. The measures most commonly used in the treatment of DN include strict control of hyperglycemia and blood pressure, as well as the use of renin-angiotensin-aldosterone system (RAS) blockers.[5,6] However, these treatments are not effective at preventing disease progression, and there is a pressing need for the development of novel therapeutics that inhibit the progression of DN.

Mounting evidence suggests that the development of DN is associated with the concomitant activation of several stress-sensitive signal pathways, including mitogen-activated protein kinase (MAPK) cascades. As principal members of the MAPK family, extracellular signal-regulated kinases 1 and 2 (ERK1/2) have been shown to play a crucial role in cell proliferation and extracellular matrix protein synthesis.[7] Previous studies confirmed that ERK1/2 is activated in glomeruli of diabetic rats and mesangial cells cultured under high-glucose conditions.[8,9] The inhibition of ERK1/2 and associated downstream cascades confers a protective effect against DN.[10,11]

Traditional Chinese medicines (TCM) have long been applied for intervention in different diseases.[12–15] In particular, *Astragalus membranaceus (Fisch) Bge* has been widely used in TCM for thousands of years; astragaloside IV (AS-IV) is one of its most important and active constituent compounds. Increasing *in vitro* and *in vivo* evidence suggests that AS-IV could alleviate kidney injury.[16,17] In addition, several reports have suggested that AS-IV may exert beneficial effects in DN through these pleiotropic activities.[18] However, the exact molecular mechanisms that underpin these effects remain unclear. Recent studies have demonstrated that the renoprotective effects mediated by AS-IV are associated with MAPK pathways.[19] Our previous study demonstrated that AS-IV can suppress the activation of ERK1/2 in db/db mice.[18] To the best of our knowledge, there have been no reports of the activation of ERK1/2 and its up- and downstream targets in the streptozotocin (STZ)-induced early-stage DN model. In the present

study, we investigated the renoprotective mechanisms of AS-IV by inhibiting activation of MEK1/2-ERK1/2-RSK2 signaling in STZ-induced type 1 DN.

Materials and methods

Animal model and drug treatment

Healthy male C57BL/6 mice (5 to 6 weeks old) weighing 16 to 18 g were purchased from the Guangdong Medical Laboratory Animal Center. All animal studies were performed in accordance with the NIH statements regarding "Principles of Laboratory Animal Care" and were approved by the Guangzhou University of Chinese Medicine Institutional Animal Care and Use Committee. Mice were housed at constant room temperature ($20 \pm 1^{\circ}C$) under a controlled 12:12-hour light-dark cycle; they were fed a standard diet and given free access to water. Mice were randomly divided into the following three groups (n=8 to 10 per group): control mice (control group), STZ-induced diabetic mice, and diabetic mice who were fed a diet supplemented with AS-IV (AS-IV-treated mice). Experimental diabetes was induced in mice, following 4 hours of fasting, by a single intraperitoneal injection (200 mg/kg) of streptozotocin (STZ, Sigma-Aldrich, St. Louis, MO, USA) dissolved in 0.1 M citrate buffer (pH 4.2). Normal control mice were intraperitoneally injected with an equal volume of vehicle. At 1 week after STZ injection, tail vein blood was collected for blood glucose measurements. Mice with fasting blood glucose concentrations >16.7 mmol/L were considered diabetic mice. AS-IV administration was initiated at 1 week after STZ injection. AS-IV, purchased from Cheng Du Con Bon Biotech Co., LTD (Chengdu, China), was added to the standard chow at 5 g/kg diet. The treatment period lasted for 8 weeks.

Metabolic parameters and tissue preparation

Every two weeks, each mouse was weighed and blood samples were obtained by tail vein puncture for blood glucose measurements by using a blood glucose meter (Roche, Basel, Switzerland). Mice were kept in metabolic cages (Tecniplast S.p.a, Buguggiate, Italy) to facilitate the collection of 24-hour urine samples at 4 and 8 weeks of treatment. At the end of 8 weeks of treatment, mice were sacrificed; blood samples and kidney tissues were harvested immediately. Urine and serum biochemical parameters, including blood urea nitrogen (BUN), serum creatinine (Scr), urine creatinine (Ucr), alanine aminotransferase (ALT), aspartate aminotransferase (AST), albumin (ALB), total protein (TP), triglyceride (TG), high-density lipoprotein cholesterol (HDL-C), low-density lipoprotein cholesterol (LDL-C), urinary glucose, and urinary N-acetyl-β-d-glucosaminidase (NAG) were measured by using a Roche automatic biochemical analyzer. Urinary albumin to creatinine ratio (UACR) was calculated and presented as urine albumin (mg) divided by Ucr (g). At the time of sacrifice, excised kidneys were weighed and rinsed in phosphate buffer solution. The left kidney was sliced into two parts to facilitate histopathology analyses. The right kidney was immediately snap-frozen in liquid nitrogen and stored at $-80^{\circ}C$ for additional analyses.

Enzyme-linked immunosorbent assay (ELISA)

Urinary albumin (Bethyl Laboratories, Montgomery, TX, USA), urinary neutrophil gelatinase-associated lipocalin (NGAL; R&D Systems, Minneapolis, MN, USA), urinary transforming growth factor-beta 1 (TGF-β1; R&D Systems), and serum insulin (Merck, Darmstadt, Germany) ELISA kits

were used in accordance with the manufacturers' instructions.

Light microscopy

Kidneys were fixed with 10% buffered formalin, embedded in paraffin, cut into 2-μm sections and stained with periodic acid-Schiff (PAS) reagent to evaluate glomerular and tubular alterations. For each section, 30 to 60 renal glomerular tuft areas (GTA), 30 renal glomerular mesangial matrix areas, 80 to 110 renal tubular areas and tubular lumen areas (axial ratio less than 1.5) were measured by using NIS-Elements imaging software Version 4.10 (Nikon Corporation, Tokyo, Japan).

Electron microscopy

After incubation on ice, the renal cortex was cut into 1-mm^3 sections; these sections ("tissue fragments") were immediately fixed in 2.5% glutaraldehyde. Tissue fragments were postfixed with 1% osmic acid, dehydrated with graded ethanol, and then embedded in Epon. Ultrathin sections (50 to 70 nm) were subsequently stained with uranyl acetate and lead citrate, then examined by electron microscopy (EM). ImageJ software (National Institutes of Health, Bethesda, MD, USA) was used to analyze images collected by EM (JEM-1400, JEOL Ltd., Tokyo, Japan) under 12,000×magnification. Glomerular basement membranes (GBM) and tubular basement membranes (TBM) (10 to 13 photographs per sample, n=3 per group) were measured by using the grid intersect method. Average podocyte foot process width (FPW) was measured by using the following formula: $FPW = (\pi/4) \times (\Sigma GBM\ length/\Sigma\ number\ of\ foot\ process)$. The FPW (6 to 13 photographs per sample, n=3 per group) values were subsequently presented in nanometers (nm).

Western blotting analysis

Snap-frozen renal cortical tissue was homogenized in lysis buffer as previously described.[20–22] Equal amounts of sample (20 μg) were separated on 10% sodium dodecyl sulfate (SDS)/polyacrylamide gels, then transferred to polyvinylidene difluoride (PVDF) membranes (Bio-Rad Laboratories, Hercules, CA, USA). Non-specific binding was blocked by incubating the membranes at room temperature for 1 hour with 5% non-fat milk in Tris-buffered saline (TBS). The membranes were subsequently incubated overnight at 4°C with the following primary antibodies: p-ERK (Thr202/Tyr204) (#4370, Cell Signaling Technology® (CST), Danvers, MA, USA), ERK1/2 (#4695, CST), p-RSK2 (Ser227) (#3556, CST), RSK2 (#5528, CST), p-MEK1/2 (ser217/221) (#9154, CST), MEK1/2(47E6) (#9126, CST). β-actin (Sigma-Aldrich) was used as a loading control. After washing three times with TBS, membranes were incubated with horseradish peroxidase-conjugated secondary antibodies for 1 hour at room temperature with shaking. Protein bands were visualized and analyzed by using a ChemiDoc™ MP Imaging System (Bio-Rad Laboratories). Results were expressed as the integrated optical density relative to β-actin.

Statistical analysis

Statistical analyses were conducted by using SPSS 17.0 software (SPSS Inc., Chicago, IL, USA). All data were expressed as means ± standard deviation (SD). Statistically significant differences between two groups were evaluated by using Student's t-test. Differences between multiple groups were determined by one-way ANOVA analysis of variance, followed by post hoc Tukey test. Data were considered to be statistically significant if $P < 0.05$.

Results

AS-IV significantly attenuates albuminuria in diabetic mice

Compared with control mice, 24-hour urinary albumin excretion and UACR were significantly increased in diabetic mice at 4 and 8 weeks (both $P < 0.001$; Figure 1a-b). Following treatment with AS-IV for 4 weeks, 24-hour urinary albumin excretion ($P<0.01$) and UACR ($P<0.05$) were markedly reduced; this effect continued through 8 weeks of treatment with AS-IV (both $P < 0.05$; Figure 1a-b).

Physiological parameters and serum levels of biochemical markers

As shown in Table 1, STZ-induced diabetic mice exhibited polydipsia, polyuria, polyphagia, and increased fecal production, following treatment with STZ. AS-IV administration did not relieve these symptoms. Diabetic mice exhibited elevated blood glucose, compared with control mice, during the entire study period ($P < 0.001$ for all time points; Figure 2a). At 8 weeks of treatment with AS-IV, diabetic mice demonstrated significantly higher urinary glucose and lower serum insulin, compared with control mice (both $P < 0.001$; Figure 2b-c). However, no significant differences were found in these parameters between diabetic mice and AS-IV-treated mice (Figure 2a-c). Levels of Scr and BUN in diabetic mice were substantially higher than in control mice. AS-IV administration significantly reduced Scr levels after 8 weeks of treatment ($P < 0.05$; Table 2). Compared with control mice, diabetic mice exhibited significantly higher TG ($P < 0.05$) and slightly lower HDL-C. Treatment with AS-IV resulted in an increase in HDL-C ($P < 0.01$), but no change in TG. In addition, no difference in LDL-C was observed among the three groups at 8 weeks after AS-IV administration (Table 2).

Effects of AS-IV on glomerular hypertrophy and injury in diabetic mice

Diabetic mice exhibited decreased body weight, compared with control mice, after STZ induction ($P < 0.001$ for all time points; Figure 3a). However, no difference in body weight was detected between diabetic mice and AS-IV-treated mice (Figure 3a).

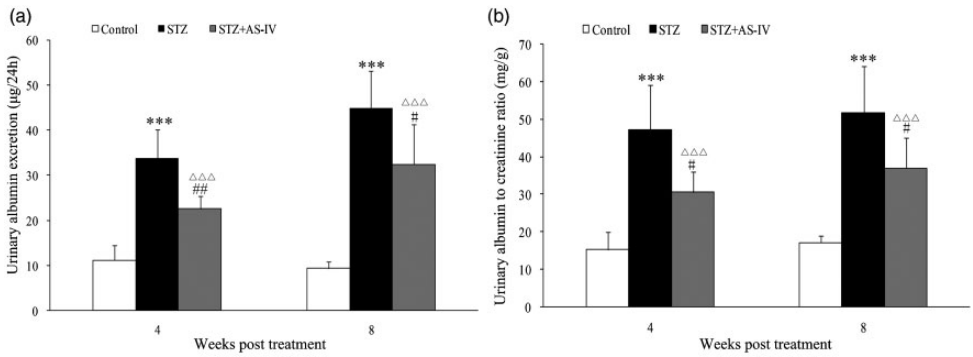

Figure 1. Astragaloside IV (AS-IV) reduced the albuminuria in diabetic mice. Effects of AS-IV on (a) urinary albumin excretion and (b) urinary albumin to creatinine ratio (UACR) after 4 and 8 weeks of treatment. Results are represented as mean ± SD (n = 6 per group). $^{***}P < 0.001$ between the control and the streptozotocin (STZ) group; $^{\#}P < 0.05$ and $^{\#\#}P < 0.01$ between the STZ and the STZ+ AS-IV groups. $^{\triangle\triangle\triangle}P < 0.001$ between the control and the STZ+ AS-IV groups.

Table 1. Metabolic characteristics of experimental mice

Weeks	Group	Food consumption (g/24 h)	Water consumption (mL/24 h)	Urine output (ml/24 h)	Feces production (g/24 h)
0	Control	1.66±0.09	2.98±0.16	1.39±0.10	0.63±0.03
	STZ	4.23±0.45***	15.63±4.33**	12.63±4.33**	1.73±0.79*
	STZ+AS-IV	3.73±1.16	13.83±5.20	11.08±3.88	1.25±0.53
4	Control	260±0.26	5.75±0.74	2.05±1.06	0.99±0.06
	STZ	4.27±0.84***	21.23±4.83***	17.75±2.95***	2.08±1.77
	STZ+AS-IV	4.50±0.47	23.45±2.22	19.67±3.46	2.10±0.85
8	Control	2.14±0.37	4.84±0.39	1.82±0.09	0.85±0.10
	STZ	5.72±0.96***	25.32±3.54***	23.25±3.40***	2.02±0.75**
	STZ+AS-IV	5.15±1.11	26.85±4.97	24.41±5.77	2.22±0.72

Results are expressed as the mean ± standard deviation (n = 6/each group). *$P < 0.05$, **$P < 0.01$, and ***$P < 0.001$ vs. normal control group. Streptozotocin (STZ), astragaloside IV (AS-IV).

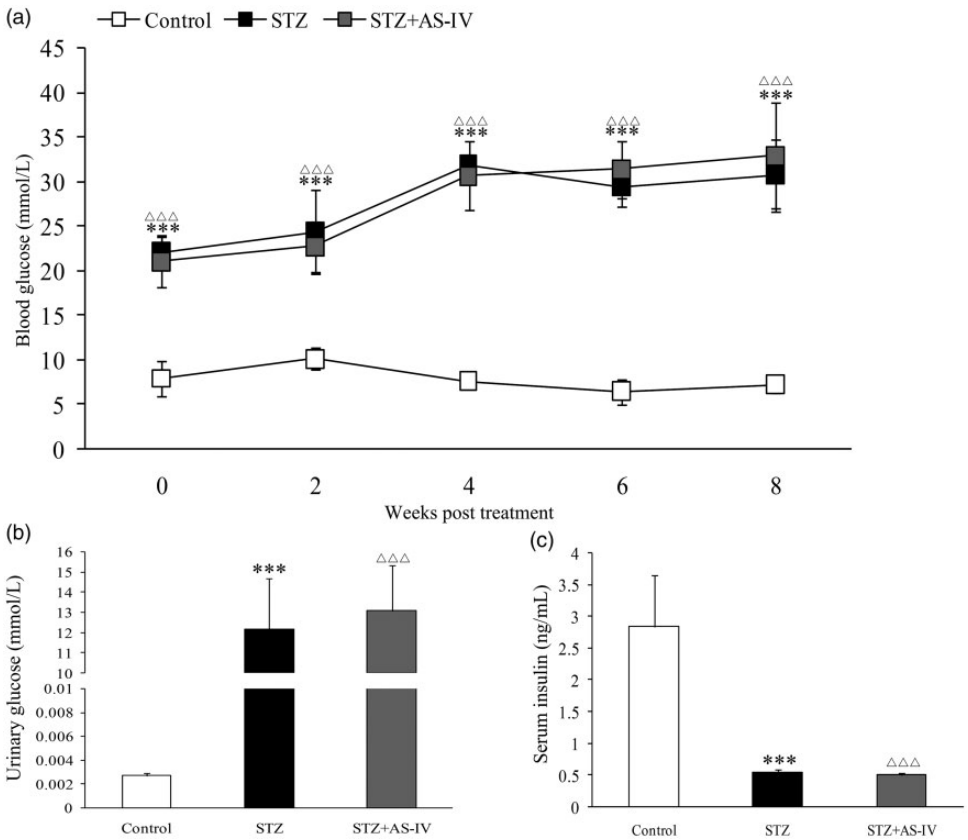

Figure 2. Astragaloside IV (AS-IV) had no effect on fasting blood glucose, urinary glucose and serum insulin in diabetic mice. Effects of AS-IV on blood glucose levels throughout the study (a). Effects of AS-IV on urinary glucose (b) and serum insulin (c) after 8 weeks of treatment. Results are represented as mean ± SD (n = 6 per group). ***$P < 0.001$ between the control and the streptozotocin (STZ) groups. $^{\triangle\triangle\triangle}P < 0.001$ between the control and the STZ+ AS-IV groups.

Table 2. Serum levels of biochemical parameters in various groups after 8 weeks

Variables	Control	STZ	STZ+AS-IV
BUN (mmol/L)	12.80±1.04	17.03±2.91**	17.25±3.79
Scr (μmol/L)	12.67±1.37	15.50±4.09	11.17±2.23$^{\#}$
TG (mmol/L)	1.46±0.34	2.66±1.25*	2.85±1.27
HDL-C (mmol/L)	2.20±0.14	1.96±0.24	2.68±0.33$^{\#\#}$
LDL-C (mmol/L)	0.21±0.05	0.29±0.11	0.30±0.10
ALT (U/L)	36.33±6.31	72.63±14.49***	75.87±14.08
AST (U/L)	151.35±45.11	218.85±28.89*	223.15±52.23
ALB (g/L)	40.83±1.20	32.62±1.42***	30.12±4.26
TP (g/L)	61.68±0.76	50.42±2.58***	49.58±4.62

Results are expressed as the mean ± standard deviation (n = 6/each group). *$P < 0.05$, **$P < 0.01$ and ***$P < 0.001$ vs. normal control group. $^{\#}P < 0.05$ and $^{\#\#}P < 0.01$ vs. untreated diabetic group. Streptozotocin (STZ), astragaloside IV (AS-IV), blood urea nitrogen (BUN), serum creatinine (Scr), urine creatinine (Ucr), alanine aminotransferase (ALT), aspartate aminotransferase (AST), albumin (ALB), total protein (TP), triglyceride (TG), high-density lipoprotein cholesterol (HDL-C), low-density lipoprotein cholesterol (LDL-C).

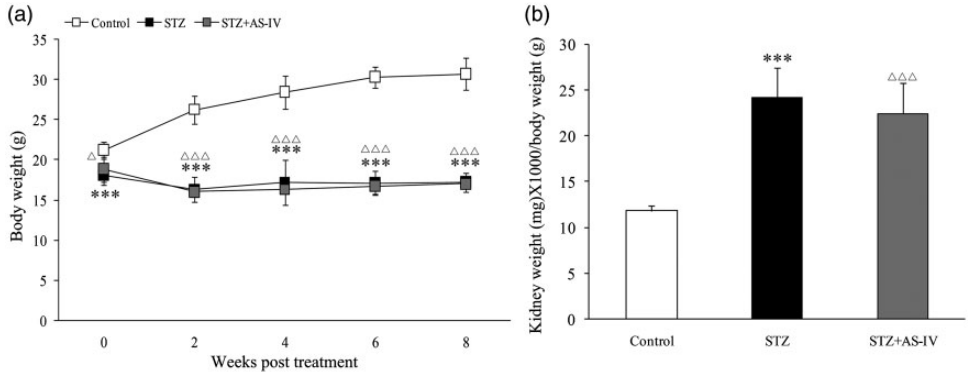

Figure 3. Astragaloside IV (AS-IV) had no effect on body weight and kidney weight in diabetic mice. Effects of AS-IV on body weight throughout the study (a). Effects of AS-IV on kidney weight after 8 weeks of treatment (b). ***$P < 0.001$ between the control and the streptozotocin (STZ) groups. $^{\triangle}P < 0.05$ and $^{\triangle\triangle\triangle}P < 0.001$ between the control and the STZ+ AS-IV groups.

Kidney weight (expressed as kidney weight/body weight) was significantly greater in diabetic mice than in normal mice at the end of the study ($P < 0.001$; Figure 3b). However, kidney weight was only slightly reduced after 8 weeks of treatment with AS-IV, compared with kidney weight in untreated diabetic mice (Figure 3b). At 8 weeks, diabetic mice exhibited larger GTA, higher mesangial matrix ratios, thicker GBM, and greater FPW, compared with control mice ($P < 0.01$ for GTA, $P < 0.05$ for all others; Figure 4a-d). AS-IV treatment significantly ameliorated the diabetic changes in GTA, mesangial matrix, and FPW ($P < 0.05$ for all; Figure 4a-b, d). However, AS-IV had no obvious effect on GBM (Figure 4c). PAS staining and EM were used to evaluate these characteristics in each group (Figure 4e).

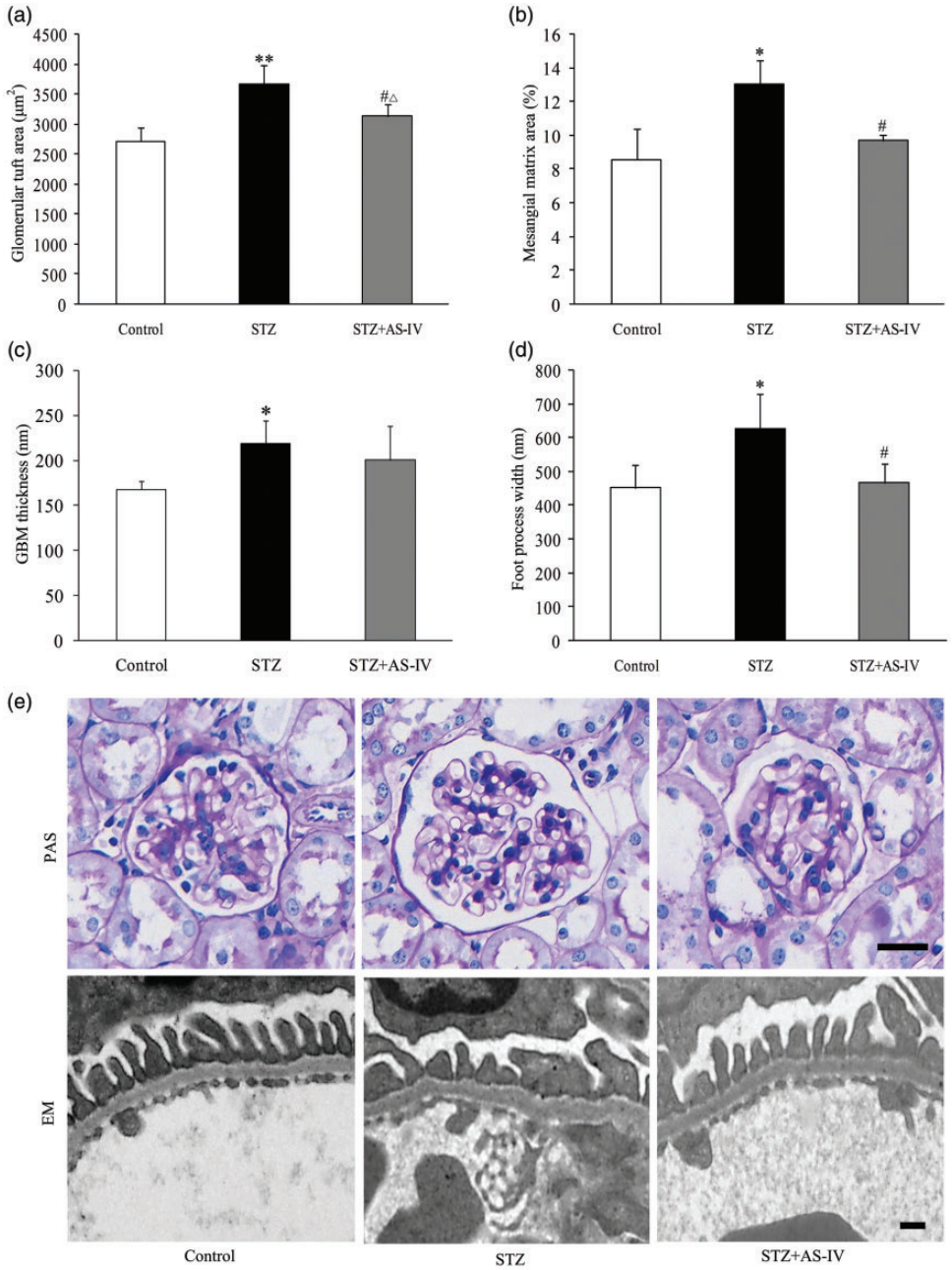

Figure 4. Astragaloside IV (AS-IV) attenuated glomerular tuft areas (GTA), mesangial matrix and foot process width (FPW), but did not affect glomerular basement membranes (GBM) in diabetic mice. Effects of AS-IV on GTA (a), mesangial matrix (b), GBM (c) and FPW (d) after 8 weeks of treatment. Periodic acid-Schiff (PAS) staining and electron microscopy (EM) images were used to depict these characteristics for each group (e). Scale bars, 25 μm for PAS images, 200 nm for EM. Results are represented as mean ± SD (n = 3–6 per group). $^{*}P < 0.05$ and $^{**}P < 0.01$ between the control and the streptozotocin (STZ) group. $^{\#}P < 0.05$ between the STZ and the STZ+ AS-IV groups. $^{\triangle}P < 0.05$ between the control and the STZ+ AS-IV groups.

Effects of AS-IV on tubular injury in diabetic mice

Compared with control mice, diabetic mice showed a significant increase in urinary levels of NGAL, NAG, and TGF-β1 at 8 weeks ($P < 0.001$ for all; Figure 5a-c). AS-IV administration resulted in a significant reduction in urinary NGAL and NAG (both $P < 0.05$); no significant differences in TGF-β1 were found after 8 weeks of treatment (Figure 5c). Histomorphological changes in the proximal tubules of the kidneys were also investigated. Compared with control mice, the proximal tubular area and lumen were slightly larger and the TBM was thicker ($P < 0.05$) in diabetic mice (Figure 5d-f). AS-IV treatment reduced these histopathological alterations, although no statistically significant differences were found in TBM and proximal tubular lumen (Figure 5d-f). PAS staining and EM were used to evaluate these characteristics in each group (Figure 5g).

AS-IV inhibits renal cortical overexpression of MEK1/2-ERK1/2-RSK2 signaling pathway proteins in diabetic mice

Expression levels of p-MEK1/2 (ser217/221), p-ERK1/2(Thy202/Tyr204), and p-RSK2 (Ser227) were significantly upregulated in diabetic model mice, compared with control mice ($P < 0.01$ for all; Figure 6a-f). However, total RSK2, ERK1/2, and MEK1/2 protein levels did not substantially change, as indicated by western blot analysis (Figure 6a, c, e). In AS-IV-treated mice, activation of these proteins was significantly inhibited after 8 weeks ($P < 0.01$ for all; Figure 6a-f).

AS-IV does not cause apparent toxicity to the liver

Diabetic mice showed significantly higher ALT ($P < 0.001$) and AST ($P < 0.05$), and significantly lower ALB and TP (both $P < 0.001$), compared with control mice. There were no significant differences in these parameters between diabetic mice and AS-IV-treated mice (Table 2), which indicates that AS-IV did not cause apparent toxicity to the liver.

Discussion

In this study, we demonstrated that AS-IV exerts renoprotection in STZ-induced DN, and that the effect might be partially associated with inhibition of MEK1/2-ERK1/2-RSK2 signaling.

A strong correlation has been reported between hyperglycemia and the progression of DN.[23] Strict glycemic control can significantly reduce the risk of developing microalbuminuria and overt DN.[23] Several studies have demonstrated that AS-IV reduces blood glucose levels in STZ-induced diabetic models.[24,25] However, in our study, and in several studies performed by other groups, AS-IV had no hypoglycemic effect on STZ-induced diabetic models.[26,27] These conflicting results could be related to several possible factors, including AS-IV dosage, duration of AS-IV treatment, and variations among the diabetes models that were used in each study.[28] Thus, our study suggested that the renoprotective effect of AS-IV is independent of glucose control.

Microalbuminuria is a strong prognostic indicator for the progression of early DN. It is widely accepted that the underlying pathophysiological mechanisms that underpin the role of albuminuria in DN include the occurrence of structural abnormalities, such as morphologic changes in podocytes, mesangial matrix expansion, and GBM thickening.[29] Mesangial matrix expansion occurs in DN patients before the onset of clinical manifestations.[30] The degree of mesangial expansion correlates with the occurrence of glomerulosclerosis and reduced renal function.[31] Inhibition of

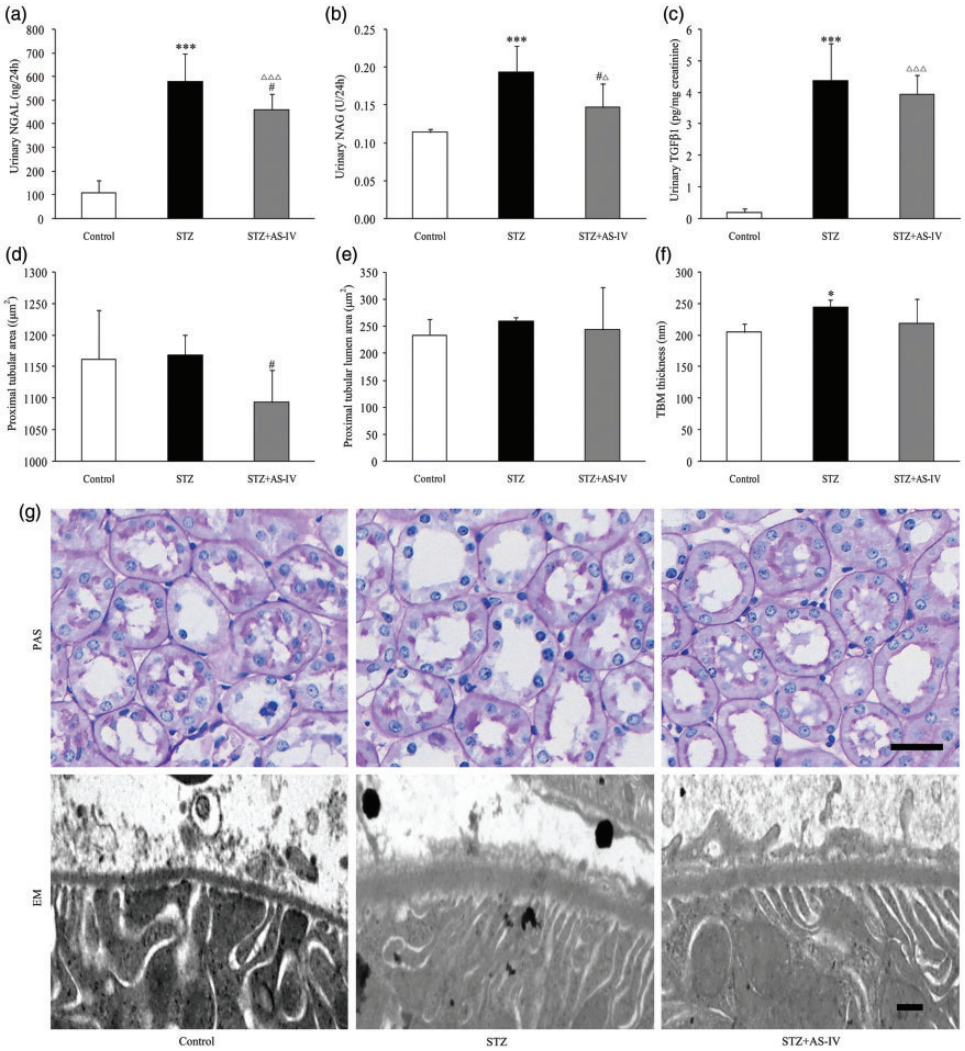

Figure 5. Astragaloside IV (AS-IV) decreased urinary N-acetyl-beta-D-glucosaminidase (NGAL), neutrophil gelatinase-associated lipocalin (NAG) and transforming growth factor-beta 1 (TGF-β1) in diabetic mice, reduced proximal tubular area, but did not affect proximal tubular lumen area and tubular basement membranes (TBM). Effects of AS-IV on urinary NGAL (a), NAG (b), TGF-β1 (c), proximal tubular area (d), proximal tubular lumen area (e) and TBM (f) after 8 weeks of treatment. The representative images of tubular periodic acid-Schiff (PAS) staining and TBM are shown in g. Scale bars, 25 μm for PAS images, 200 nm for electron microscopy (EM). Data are represented as mean ± SD (n = 3–6 per group). $^{*}P < 0.05$ and $^{***}P < 0.001$ between the control and the streptozotocin (STZ) group. $^{\#}P < 0.05$ between the STZ and the STZ+ AS-IV groups. $^{\triangle}P < 0.05$ and $^{\triangle\triangle\triangle}P < 0.001$ between the control and the STZ+ AS-IV groups.

mesangial expansion is considered a potential target in the prevention and delayed onset of DN.[32] In our study, we observed that AS-IV significantly reduces mesangial expansion caused by DN. Podocytes play a crucial role in the maintenance of the glomerular filtration barrier and in glomerular structural integrity.[33–36] Increasing evidence

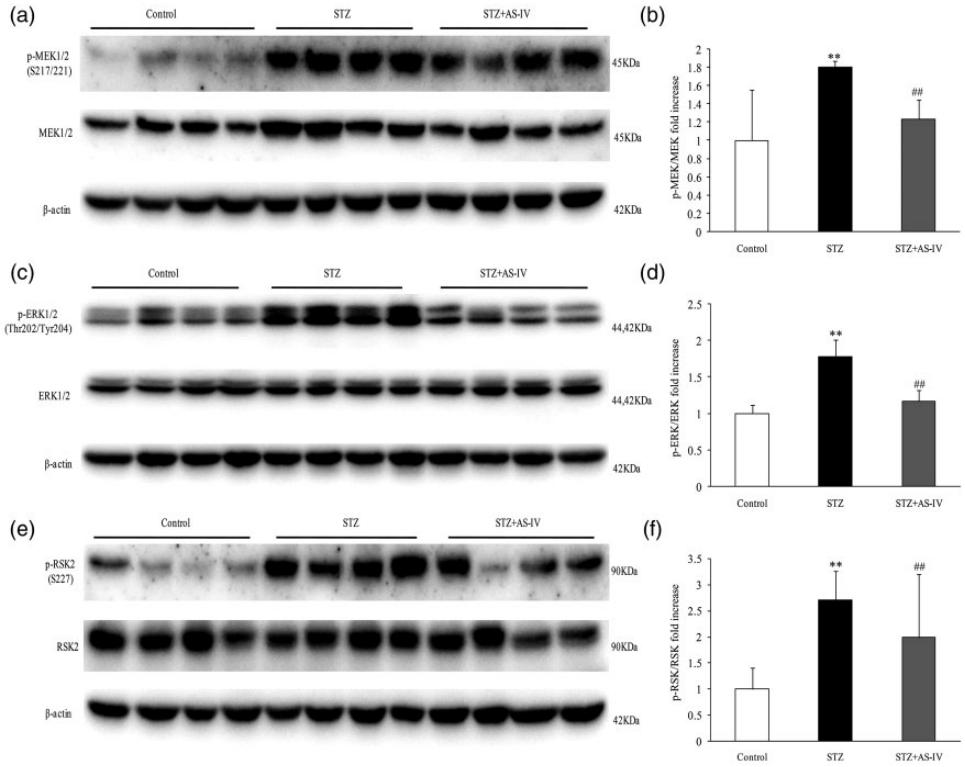

Figure 6. Astragaloside IV (AS-IV) inhibited the activation of MEK1/2, ERK1/2 and RSK2 in the renal cortex of diabetic mice. Effects of AS-IV on the expression of p-MEK1/2 (b), p-ERK1/2 (d), and p-RSK2 (f) in the renal cortex of diabetic mice after 8 weeks of treatment. Representative western blots are shown for total and phosphorylated MEK1/2 (a), ERK1/2 (c) and RSK2 (e). Data are represented as mean ± SD (n = 4 per group). $^{**}P < 0.01$ between the control and the streptozotocin (STZ) group. $^{\#\#}P < 0.01$ between the STZ and the STZ+AS-IV groups.

suggests that a reduction in the number of podocytes may lead to the development of proteinuria in both type 1 and type 2 diabetes.[37] This loss of podocytes would require the residual cells to cover a larger area of the GBM, which could then cause foot process widening. Widening of foot processes has been confirmed to correlate directly with microalbuminuria in type 1 DN.[38] Previous studies have indicated that AS-IV treatment ameliorated podocyte loss in STZ-induced diabetic rats.[39] However, it is unclear whether AS-IV plays a role in podocyte FPW. In our study, we observed that AS-IV significantly reduced FPW. Tubular injury has been reported as a critical component in the pathogenesis of early DN.[40] Several studies previously reported that AS-IV has a protective effect on tubular injury.[41,42] However, there is little evidence regarding the effectiveness of AS-IV on tubular injury in STZ-induced diabetic mice. In the present study, specific tubular injury biomarkers, including NAG, NGAL, and TGF-β1, were reduced following AS-IV treatment. Consistent with these results, AS-IV ameliorated the increase in the proximal tubular area in diabetic mice.

We further investigated possible molecular mechanisms underlying the renoprotective

effects associated with AS-IV treatment. Mesangial matrix expansion is largely due to the accumulation of extracellular matrix (ECM) proteins. Excessive accumulation of ECM occurs in early DN and this phenomenon contributes greatly to renal glomerular sclerosis and interstitial fibrosis.[43] Several signaling pathways are involved in ECM production, including TGF-β/Smad, Wnt/β-catenin, PI3K/Akt, and MAPK.[21,36,44] The MAPK family comprises three major subgroups, namely ERK, c-jun N-terminal kinases (JNK), and p38 MAPK (p38).[45] Of these, the activated ERK1/2 pathway plays a major role in the regulation of cell growth, survival, and differentiation.[46] This pathway has a well-characterized role in regulating ECM expression. Previous studies reported that renal ERK1/2 activity was significantly increased both in DN animal models and cultured renal cells.[47,48] ERK phosphorylation was also confirmed to be associated with the extent of glomerular lesions in human DN.[49] Furthermore, treatments used to inhibit increased p-ERK1/2 levels have been shown to ameliorate DN.[50] Consistent with previous studies, we found that p-ERK1/2 is upregulated in the kidneys of STZ-induced diabetic mice. In addition, up- and downstream modulators of p-ERK1/2, including p-MEK1/2 and p-RSK2, were increased. AS-IV has been reported to exhibit antifibrotic effects by inhibiting TGF-β1-induced phosphorylation of ERK1/2 in cultured mouse renal fibroblasts.[51] However, it is not clear whether AS-IV treatment can inhibit ERK1/2 activation in STZ-induced diabetic mice. In the present study, analysis of the underlying mechanisms elicited by AS-IV treatment showed that AS-IV dramatically suppressed phosphorylation of ERK1/2, MEK1/2, and RSK2 in STZ-induced diabetic mice. These results indicate that renoprotection caused by AS-IV treatment might be partially associated with inhibition of MEK1/2-ERK1/2-RSK2 signaling.

In conclusion, this study demonstrated that AS-IV treatment reduced urinary albumin excretion and ameliorated structural and functional abnormalities associated with diabetic kidneys in the STZ-induced diabetic mouse model. The molecular mechanisms underlying the renoprotective effects of AS-IV might be partially associated with reduced ECM deposition through inhibition of MEK1/2-ERK1/2-RSK2 signaling. Taken together, these novel findings suggest that AS-IV might serve as an alternative therapeutic agent in the treatment of early DN.

Declaration of conflicting interest

The authors declare that there is no conflict of interest.

Funding

This study was supported by grants from the National Natural Science Foundation of China (81673794, 81373565), Natural Science Foundation of Guangdong Province (2015A030313883), and Shenzhen Science and Technology Project (JCYJ20160330171116798, JCYJ20150401163247228).

References

1. Ritz E, Rychlik I, Locatelli F, et al. End-stage renal failure in type 2 diabetes: A medical catastrophe of worldwide dimensions. *Am J Kidney Dis* 1999; 34: 795–808.
2. Zhang Z, Mao J, Chen H, et al. Removal of uremic retention products by hemodialysis is coupled with indiscriminate loss of vital metabolites. *Clin Biochem* 2017; 50: 1078–1086.
3. Chen H, Chen L, Liu D, et al. Combined clinical phenotype and lipidomic analysis reveals the impact of chronic kidney disease on lipid metabolism. *J Proteome Res* 2017; 16: 1566–1578.
4. Cooper ME. Pathogenesis, prevention, and treatment of diabetic nephropathy. *Lancet* 1998; 352: 213–219.

5. National Kidney Foundation. KDOQI clinical practice guideline for diabetes and CKD: 2012 update. *Am J Kidney Dis* 2012; 60: 850–886.
6. Nelson RG and Tuttle KR. Prevention of diabetic kidney disease: negative clinical trials with renin-angiotensin system inhibitors. *Am J Kidney Dis* 2010; 55: 426–430.
7. Seger R and Krebs EG. The MAPK signaling cascade. *Faseb J* 1995; 9: 726–735.
8. Awazu M, Ishikura K, Hida M, et al. Mechanisms of mitogen-activated protein kinase activation in experimental diabetes. *J Am Soc Nephrol* 1999; 10: 738–745.
9. Haneda M, Araki S, Togawa M, et al. Mitogen-activated protein kinase cascade is activated in glomeruli of diabetic rats and glomerular mesangial cells cultured under high glucose conditions. *Diabetes* 1997; 46: 847–853.
10. Zhou Y, Li JS, Zhang X, et al. Ursolic acid inhibits early lesions of diabetic nephropathy. *Int J Mol Med* 2010; 26: 565–570.
11. Sedeek M, Gutsol A, Montezano AC, et al. Renoprotective effects of a novel Nox1/4 inhibitor in a mouse model of Type 2 diabetes. *Clin Sci (Lond)* 2013; 124: 191–202.
12. Zhao Y. Traditional uses, phytochemistry, pharmacology, pharmacokinetics and quality control of Polyporus umbellatus (Pers.) Fries: A review. *J Ethnopharmacol* 2013; 149: 35–48.
13. Tian T, Chen H and Zhao Y. Traditional uses, phytochemistry, pharmacology, toxicology and quality control of Alisma orientale (Sam.) Juzep: A review. *J Ethnopharmacol* 2014; 158: 373–387.
14. Chen H, Tian T, Miao H, et al. Traditional uses, fermentation, phytochemistry and pharmacology of Phellinus linteus: A review. *Fitoterapia* 2016; 113: 6–26.
15. Zhang Z, Wei F, Vaziri ND, et al. Metabolomics insights into chronic kidney disease and modulatory effect of rhubarb against tubulointerstitial fibrosis. *Sci Rep* 2015; 5: 14472.
16. Gui D, Huang J, Liu W, et al. Astragaloside IV prevents acute kidney injury in two rodent models by inhibiting oxidative stress and apoptosis pathways. *Apoptosis* 2013; 18: 409–422.
17. Wang L, Chi YF, Yuan ZT, et al. Astragaloside IV inhibits renal tubulointerstitial fibrosis by blocking TGF-beta/Smad signaling pathway in vivo and in vitro. *Exp Biol Med (Maywood)* 2014; 239: 1310–1324.
18. Sun H, Wang W, Han P, et al. Astragaloside IV ameliorates renal injury in db/db mice. *Sci Rep* 2016; 6: 32545.
19. Zheng R, Deng Y, Chen Y, et al. Astragaloside IV attenuates complement membranous attack complex induced podocyte injury through the MAPK pathway. *Phytother Res* 2012; 26: 892–898.
20. Sun H, Ge N, Shao M, et al. Lumbrokinase attenuates diabetic nephropathy through regulating extracellular matrix degradation in Streptozotocin-induced diabetic rats. *Diabetes Res Clin Pract* 2013; 100: 85–95.
21. Wang M, Chen D, Wang M, et al. Poricoic acid ZA, a novel RAS inhibitor, attenuates tubulo-interstitial fibrosis and podocyte injury by inhibiting TGF-β/Smad signaling pathway. *Phytomedicine* 2017; 36: 243–253.
22. Zhao Y, Wang H, Cheng X, et al. Metabolomics analysis reveals the association between lipid abnormalities and oxidative stress, inflammation, fibrosis and Nrf2 dysfunction in aristolochic acid-induced nephropathy. *Sci Rep* 2015; 5: 12936.
23. Fioretto P, Bruseghin M, Berto I, et al. Renal protection in diabetes: role of glycemic control. *J Am Soc Nephrol* 2006; 17: S86–S89.
24. Lv L, Wu SY, Wang GF, et al. Effect of astragaloside IV on hepatic glucose-regulating enzymes in diabetic mice induced by a high-fat diet and streptozotocin. *Phytother Res* 2010; 24: 219–224.
25. Yu J, Zhang Y, Sun S, et al. Inhibitory effects of astragaloside IV on diabetic peripheral neuropathy in rats. *Can J Physiol Pharmacol* 2006; 84: 579–587.
26. Gui D, Huang J, Guo Y, et al. Astragaloside IV ameliorates renal injury in streptozotocin-induced diabetic rats through inhibiting NF-kappaB-mediated inflammatory genes expression. *Cytokine* 2013; 61: 970–977.
27. Wang ZS, Xiong F, Xie XH, et al. Astragaloside IV attenuates proteinuria in streptozotocin-induced diabetic nephropathy

via the inhibition of endoplasmic reticulum stress. *Bmc Nephrol* 2015; 16: 44.
28. Ding Y, Yuan S, Liu X, et al. Protective effects of astragaloside IV on db/db mice with diabetic retinopathy. *Plos One* 2014; 9: e112207.
29. Wolf G and Ziyadeh FN. Cellular and molecular mechanisms of proteinuria in diabetic nephropathy. *Nephron Physiol* 2007; 106: 26–31.
30. Ichinose K, Kawasaki E and Eguchi K. Recent advancement of understanding pathogenesis of type 1 diabetes and potential relevance to diabetic nephropathy. *Am J Nephrol* 2007; 27: 554–564.
31. Li J, Lee YS, Choi JS, et al. Roasted licorice extracts dampen high glucose-induced mesangial hyperplasia and matrix deposition through blocking Akt activation and TGF-beta signaling. *Phytomedicine* 2010; 17: 800–810.
32. Turgut F and Bolton WK. Potential new therapeutic agents for diabetic kidney disease. *Am J Kidney Dis* 2010; 55: 928–940.
33. Li JJ, Kwak SJ, Jung DS, et al. Podocyte biology in diabetic nephropathy. *Kidney Int Suppl* 2007; 72: S36–S42.
34. Chen L, Chen D, Wang M, et al. Role of RAS/Wnt/β-catenin axis activation in the pathogenesis of podocyte injury and tubulo-interstitial nephropathy. *Chem-Biol Interact* 2017; 273: 56–72.
35. Wang M, Chen D, Chen L, et al. Novel RAS inhibitors poricoic acid ZG and poricoic acid ZH attenuate renal fibrosis via a Wnt/β-catenin pathway and targeted phosphorylation of smad3 signaling. *J Agr Food Chem* 2018; 66: 1828–1842.
36. Chen H, Yang T, Wang M, et al. Novel RAS inhibitor 25-O-methylalisol F attenuates epithelial-to-mesenchymal transition and tubulo-interstitial fibrosis by selectively inhibiting TGF-β-mediated Smad3 phosphorylation. *Phytomedicine* 2018; 42: 207–218.
37. Steffes MW, Schmidt D, McCrery R, et al. Glomerular cell number in normal subjects and in type 1 diabetic patients. *Kidney Int* 2001; 59: 2104–2113.
38. Toyoda M, Najafian B, Kim Y, et al. Podocyte detachment and reduced glomerular capillary endothelial fenestration in human type 1 diabetic nephropathy. *Diabetes* 2007; 56: 2155–2160.
39. Chen J, Chen Y, Luo Y, et al. Astragaloside IV ameliorates diabetic nephropathy involving protection of podocytes in streptozotocin induced diabetic rats. *Eur J Pharmacol* 2014; 736: 86–94.
40. Vaidya VS, Niewczas MA, Ficociello LH, et al. Regression of microalbuminuria in type 1 diabetes is associated with lower levels of urinary tubular injury biomarkers, kidney injury molecule-1, and N-acetyl-beta-D-glucosaminidase. *Kidney Int* 2011; 79: 464–470.
41. Qi W, Niu J, Qin Q, et al. Astragaloside IV attenuates glycated albumin-induced epithelial-to-mesenchymal transition by inhibiting oxidative stress in renal proximal tubular cells. *Cell Stress Chaperones* 2014; 19: 105–114.
42. Wang Q, Shao X, Xu W, et al. Astragalosides IV inhibits high glucose-induced cell apoptosis through HGF activation in cultured human tubular epithelial cells. *Ren Fail* 2014; 36: 400–406.
43. Kolset SO, Reinholt FP and Jenssen T. Diabetic nephropathy and extracellular matrix. *J Histochem Cytochem* 2012; 60: 976–986.
44. Zhu L, Zhao S, Liu S, et al. PTEN regulates renal extracellular matrix deposit via increased CTGF in diabetes mellitus. *J Cell Biochem* 2016; 117: 1187–1198.
45. Balbi AP, Francescato HD, Marin EC, et al. Roles of mitogen-activated protein kinases and angiotensin II in renal development. *Braz J Med Biol Res* 2009; 42: 38–43.
46. Cobb MH. MAP kinase pathways. *Prog Biophys Mol Biol* 1999; 71: 479–500.
47. Kuo CW, Shen CJ, Tung YT, et al. Extracellular superoxide dismutase ameliorates streptozotocin-induced rat diabetic nephropathy via inhibiting the ROS/ERK1/2 signaling. *Life Sci* 2015; 135: 77–86.
48. Chen L, Yang T, Lu D, et al. Central role of dysregulation of TGF-β/Smad in CKD progression and potential targets of its treatment. *Biomed Pharmacother* 2018; 101: 670–681.

49. Sakai N, Wada T, Furuichi K, et al. Involvement of extracellular signal-regulated kinase and p38 in human diabetic nephropathy. *Am J Kidney Dis* 2005; 45: 54–65.
50. Hagiwara S, Makita Y, Gu L, et al. Eicosapentaenoic acid ameliorates diabetic nephropathy of type 2 diabetic KKAy/Ta mice: involvement of MCP-1 suppression and decreased ERK1/2 and p38 phosphorylation. *Nephrol Dial Transplant* 2006; 21: 605–615.
51. Che X, Wang Q, Xie Y, et al. Astragaloside IV suppresses transforming growth factor-beta1 induced fibrosis of cultured mouse renal fibroblasts via inhibition of the MAPK and NF-kappaB signaling pathways. *Biochem Biophys Res Commun* 2015; 464: 1260–1266.